Narrow-Line Single-Molecule Transducer between Electronic Circuits and Surface Plasmons

Michael C. Chong,[1] Gaël Reecht,[1] Hervé Bulou,[1] Alex Boeglin,[1] Fabrice Scheurer,[1] Fabrice Mathevet,[2] and Guillaume Schull[1,*]

[1]*Institut de Physique et Chimie des Matériaux de Strasbourg, UMR 7504 (CNRS—Université de Strasbourg), 67034 Strasbourg, France*

[2]*Institut Parisien de Chimie Moléculaire, Chimie des polymères, UMR 8232, CNRS—Université Pierre et Marie Curie, 94200 Ivry sur Seine, France*

(Received 12 September 2015; published 21 January 2016)

A molecular wire containing an emitting molecular center is controllably suspended between the plasmonic electrodes of a cryogenic scanning tunneling microscope. Passing current through this circuit generates an ultranarrow-line emission at an energy of ≈1.5 eV which is assigned to the fluorescence of the molecular center. Control over the linewidth is obtained by progressively detaching the emitting unit from the surface. The recorded spectra also reveal several vibronic peaks of low intensities that can be viewed as a fingerprint of the emitter. Surface plasmons localized at the tip-sample interface are shown to play a major role in both excitation and emission of the molecular excitons.

DOI: 10.1103/PhysRevLett.116.036802

Future ultrafast devices may rely on hybrid electronic-plasmonic circuitry [1,2]. A keystone for the realization of such components is the production of transducers allowing one to controllably couple electrical and plasmonic signals [3,4]. Tunneling electrons crossing the junction of a scanning tunneling microscope (STM) may act as an extremely localized excitation source for confined [5] or propagating [6–8] surface plasmons. Tailoring the properties of this source appears to be a dedicated method to controllably gate plasmonic waves [9] and to integrate nanoplasmonic architectures in electronic devices. Single molecules may act as controllable emitters capable of producing single photons [10,11] and narrow-line emission [12], two mandatory characteristics for quantum computation applications. Qiu *et al.* have demonstrated that a STM can be used to excite the luminescence of a single molecule *decoupled* from the metallic substrate by a thin insulating layer and from the tip by the vacuum [13]. Conserving these characteristics for a single molecule integrated in a hybrid electroplasmonic circuit is challenging because of the required *direct* contact to metallic electrodes, which alters the properties of the molecule and quenches its emission [14–16]. Recent works have shown that intrinsic radiative transitions may be preserved when elongated molecules are used as bridging elements [16,17]. In these examples, broad emission bands (FWHM ≥ 150 meV) are, however, observed, indicating the poor coherence of the emitted light.

Here, we report on the narrow-line emission (≈2.5 meV wide) from an electrically addressed molecular emitter connected to the plasmonic leads of a STM by short oligothiophene wires. Progressive lifting of the emitter from the substrate provides control over the linewidth of the emission which is finally limited by interactions with low energy phonons. Our fluorescence spectra also reveal vibronic features similar to Raman lines which provide a fingerprint of the molecular emitter. The detailed mechanisms that rule the complex interactions between the single-molecule emitter and localized surface plasmons is evidenced. Our results pave the way to nanoplasmonic devices integrating electrically gated molecular junctions as controllable excitation sources.

We used a low temperature (4.5 K) Omicron STM operating in an ultrahigh vacuum for the experiment. The light collection setup is described in Ref. [16]. The detection setup is composed of a grating spectrograph (Princeton Instruments Acton Series SP-2300i) connected to a liquid nitrogen cooled CCD camera (Princeton instruments PyLoN-100BR-eXcelon). Two different gratings were used, allowing for low (3.5 nm) and high (0.8 nm) spectral resolutions (details of the experimental setup can be found in the Supplemental Material, Sec. S1 [18]). The STM tips were indented in the sample to cover them with gold and to modify their nanoscale shape in order to control their plasmonic response. The Au(111) samples were sputtered with argon ions and annealed. $5,5''$-dibromo-$2,2':5',2''$-terthiophene and 5,15-(diphenyl)-10,20-(dibromo)porphyrin [see Fig. 1(a)] were successively deposited on the clean Au(111) surfaces at room temperature. As a next step, the samples were annealed at a temperature of ≈580 K in order to induce a polymerization reaction on the surface [23,24].

STM images recorded after the copolymerization procedure suggest (see details in the Supplemental Material, Sec. S2 [18]) that the formed nanowires [see, e.g., Fig. 1(b)] are composed of a nonregular succession of covalently

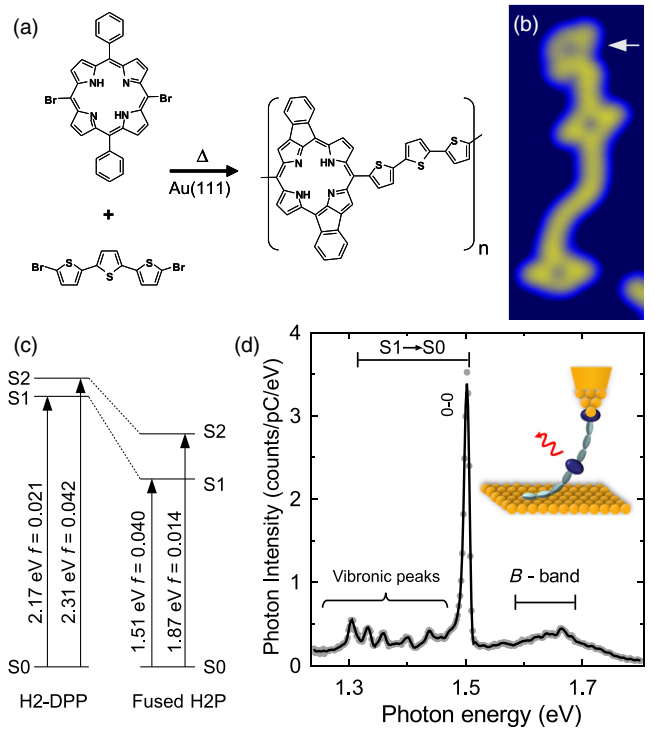

FIG. 1. STM-induced luminescence of the suspended molecular wires. (a) Sketch of the on-surface chemical reaction. (b) STM image ($3.6\times8.2\,\mathrm{nm}^2$, $I = 0.1$ nA, $V = -0.1$ V) of a copolymer composed of oligothiophene and fused-H2P units polymerized on Au(111). (c) Optical gaps of H2-DPP and fused-H2P molecules calculated using a time-dependent density functional theory (TD-DFT) approach. The calculated oscillator strengths, f, of the respective transitions are also indicated (see details about the method in the Supplemental Material, Sec. S4 [18]). (d) Characteristic light emission spectra of a copolymer wire similar to the one in (b) suspended in the STM junction ($I = 4.2$ nA, $V = 2$ V, $z = 3.2$ nm, acquisition time $t = 600$ s, low resolution grating). The emission efficiency is limited to 5×10^{-5} photons/electron and varies over orders of magnitude from junction to junction. The tip is brought into contact at the center of the fused-H2P marked by a white arrow.

linked terthiophene and H2-DPP units. A more detailed analysis demonstrates (see the Supplemental Material, Sec. S2 [18]) that the porphyrin units also undergo an intramolecular cyclodehydrogenation [25], which leads to the formation of molecules (fused-H2P), where the two peripheral phenyl rings are fused to the porphyrin macrocycle [see Fig. 1(a)]. Our time-dependent density functional theory (TD-DFT) simulations [see Fig. 1(c)] show that this cyclodehydrogenation reaction reduces the optical gap compared to the original H2-DPP.

To decouple a fused-H2P from the metallic surface, the apex of the STM tip is brought into contact with the extremity of a copolymer strand (see the Supplemental Material, Sec. S3 [18]). The tip, with the attached wire, is then retracted from the surface by a distance large enough to suspend a single fused-H2P in the junction [see the inset of Fig. 1(d)]. Electrically excited luminescence spectra obtained from such a molecular junction reveal a sharp and intense resonance at $h\nu = 1.51 \pm 0.04$ eV [26] labeled 0–0 in Fig. 1(d). Together with the vibronic peaks that appear at lower energy, this feature can be assigned to the $S1 \rightarrow S0$ transition of the fused-H2P molecule [see Fig. 1(c)]. The absence of vibronic states on the high energy side of the 0–0 line suggests that the emission is subject to Kasha's rules. A less intense component (the B band) also appears at a higher energy $h\nu \approx 1.66$ eV. Here, the agreement with the calculated $S0 \rightarrow S2$ transition (1.87 eV) is poor. Considering the oligothiophene side groups in our simulations reduces the $S0 \rightarrow S2$ transition energy to 1.74 eV, leaving the $S0 \rightarrow S1$ energy almost unchanged (see the Supplemental Material, Sec. S4 [18]). Alternatively, the B band may be attributed to radiative transitions from excited vibrational states of $S1$ to $S0$ [27,28]. Overall, the emerging picture is that the oligothiophene chains enable charge transport through the lifted copolymers while simultaneously ensuring the electronic decoupling of the central fused-H2P which acts as the optically active unit.

We will now describe how the lifetime of the molecular excited state can be controlled by progressively detaching the emitting fused-H2P from the surface [see Fig. 2(a)]. Figure 2(b) displays optical spectra of the $S1 \rightarrow S0$ band of a suspended molecular wire, similar to the one in Fig. 1(a), for tip-sample distances ranging from $z = 1.2$ nm to $z = 2.3$ nm. For the shortest distance, the emitting fused-H2P is still adsorbed on the surface and the spectrum reveals a broad feature whose width (≈100 meV) is close to the one of the localized plasmon (the black curve). At $z = 1.6$ nm a sharper feature (FWHM $= 40$ meV) appears at the energy of the 0–0 transition. The next spectra show a

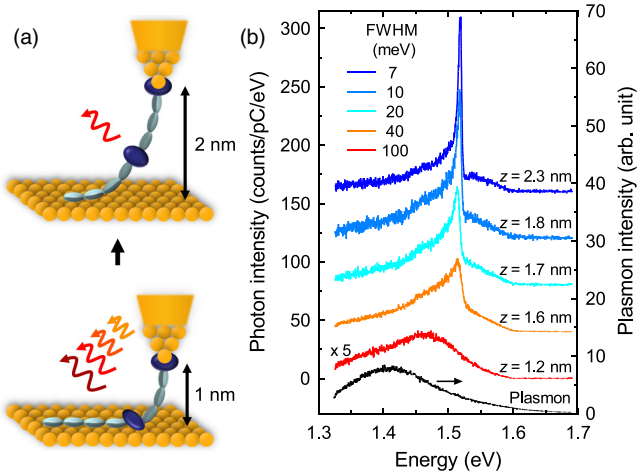

FIG. 2. Controlled emission linewidth. (a) Sketch of the experiment. (b) Light spectra as a function of the detachment of the molecular emitter from the surface ($V = 1.6$ V, $t = 60$ s, high resolution grating). The plasmon spectrum (the black curve) is acquired with the same metal tip facing the bare Au(111) surface ($V = -3$ V, $I = 9$ nA, $t = 10$ s).

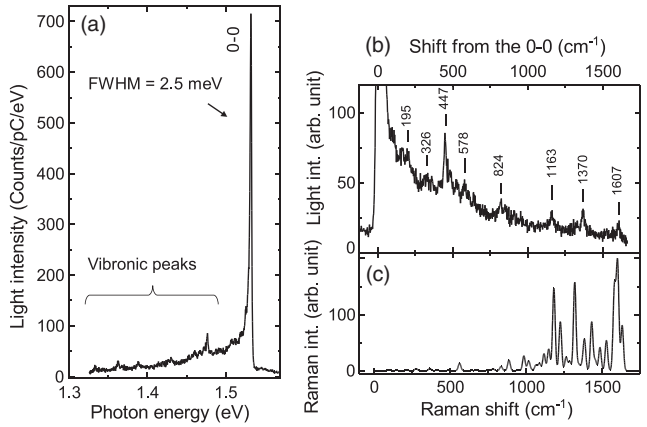

FIG. 3. Vibronic spectra as a spectroscopic fingerprint of the emitter. (a) Highly resolved light spectrum of a molecular junction ($V = 1.6$ V, $I = 0.66$ nA, $z = 1.8$ nm, $t = 60$ s, high resolution grating). (b) The same spectra, where the light intensity is represented as a function of the shift from the 0–0 line. (c) Calculated Raman intensities for the vibrational modes of the fused-H2P (see details in the Supplemental Material, Sec. S6 [18]).

progressive narrowing of this line that reaches a minimum width of 7 meV at $z = 2.3$ nm, where the emitting fused-H2P is fully detached from the surface. The 0–0 line narrowing directly reflects an increase of the excited-state lifetime of the emitter, which is controlled by tuning the coupling between the molecular and the surface electronic states. As an extreme case, the spectrum of Fig. 3(a) shows a spectral line ≈2.5 meV wide, to date the thinnest linewidth reported in a STM-induced light emission experiment. This corresponds to a lifetime of 0.26 ps and a coherence length of ≈0.15 mm, a value similar to the one of free-running laser diodes.

Finally, the 0–0 emission line appears asymmetric in all spectra, revealing a sharp edge at high energy and a shallow tail at low energy. This spectral shape may be due to the coupling between the molecular exciton and low energy phonons of the molecular chains, a phenomenon that has been studied in detail for localized excitons in carbon nanotubes [29]. Alternatively, energy losses due to excitation of low energy electron-hole pairs in the metallic electrodes may be responsible for the asymmetric line shape, a phenomenon well known in surface-enhanced Raman scattering [30]. This asymmetry effectively limits the monochromaticity of the molecular emission.

In previous STM-induced light emission experiments, vibronic features observed in optical spectra were associated with the harmonic progression of a single mode [13,27,31], and their relative intensities satisfied the Franck and Condon factors. In contrast, our spectra reveal an extremely weak intensity of the vibronic peaks compared to the 0–0 contributions and a nonlinear dispersion of the states. This suggests that each line corresponds to a given vibrational mode of the emitter, similar to what is observed in fluorescence line-narrowing spectroscopy of single molecules [32]. In Fig. 3(b) the emitted intensity is represented as a function of the shift from the 0–0 line (in cm^{-1}) and tentatively compared to [see Fig. 3(c)] the Raman intensities calculated at the DFT level for fused-H2P (see also the Supplemental Material, Secs. S5 and S6 [18]). The high energy peaks are well reproduced by the theory and can be assigned to in-plane C–C stretching modes which do not exceed ≈1700 cm^{-1} in either experiment or theory. The agreement is not as good at low energy, where the modes are strongly coupled to the environment [32]. Altogether, this provides a detailed spectroscopic fingerprint of the single-molecule emitter and its surroundings in a way that resembles recent tip-enhanced Raman spectroscopy experiments at the single-molecule level [33], but without the need for an external optical excitation.

We now turn to the exciton-plasmon interactions. The spectra of Fig. 4(a) show that the voltage onset of the emission matches the energy of the 0–0 peak, a behavior that is strikingly different from the cases where the emission is interpreted in terms of an intramolecular recombination of electrons and holes injected from the tip and the sample [13,16,27,31,34]. In these examples, both the $S1$ and $S0$ states need to be located between the Fermi levels of the electrodes, a configuration that requires a higher voltage than the energy of the $S1 \rightarrow S0$ transition. The behavior seen in Fig. 4(a) suggests another mechanism, where inelastic tunneling electrons excite localized plasmons that are finally absorbed by the molecular emitter [see Fig. 4(b)]. While similar excitation mechanisms were reported for multilayers of molecules in recent STM experiments [28,35] and were addressed theoretically [36,37], it has not yet been identified at the level of a single emitter in a STM junction.

Anger *et al.* [38] have demonstrated that, in this configuration, the emission rate γ_{em} of the molecule is as follows:

$$\gamma_{em} = \gamma_{exc} Q, \tag{1}$$

where γ_{exc} is the emitter excitation rate and Q its photon emission probability, or quantum yield. The inset of Fig. 4(a) shows the variation of γ_{em} for the 0–0 peak in Fig. 4(a) as a function of the electromagnetic field intensity at the same energy [$E^2(z, h\nu = 1.54$ eV)], as deduced from metal-metal junction measurements (see the Supplemental Material, Sec. S7 [18]). Because the tip-sample junction is unchanged, Q is constant for this set of spectra (see the Supplemental Material, Sec. S7 [18]); hence, γ_{em} only depends on the excitation rate in this case. This plot reveals that $\gamma_{exc} \propto E^2(z, h\nu)$, which is the expected behavior for an optical excitation of the emitter [38]. This is further illustrated in Figs. 4(c) and 4(d), which show that the intensity ratio between the $S1 \rightarrow S0$ and the B-band emission is modified in favor of the transition that experiences the largest plasmon intensity.

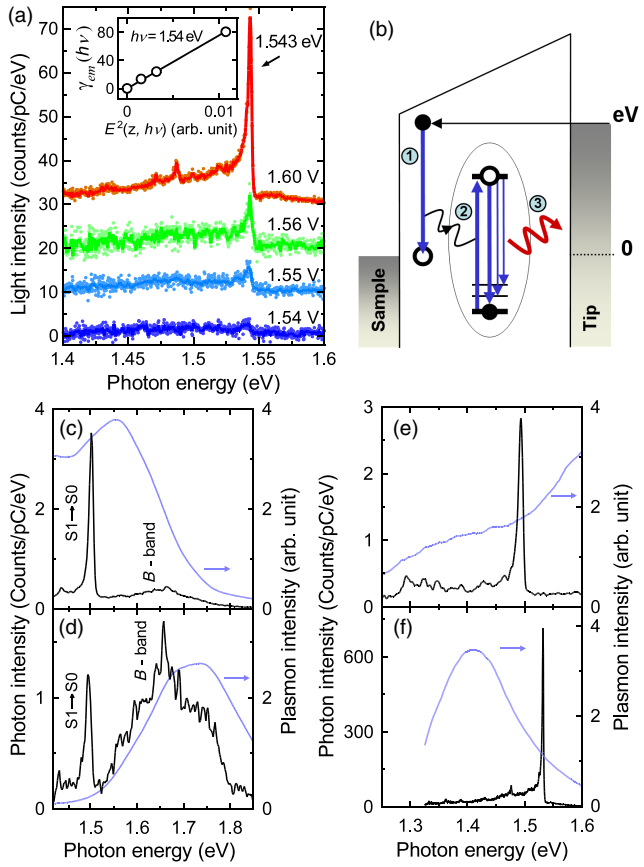

FIG. 4. Exciton-plasmon interactions. (a) Light spectra of a suspended copolymer as a function of voltage ($z = 2.1$ nm, high resolution grating) and (inset) emission rate (in counts/sec) as a function of $E^2(z, h\nu)$ at $h\nu = 1.54$ eV for the spectra at 1.6, 1.56, and 1.55 V. (b) Sketch of the luminescence mechanism: an inelastic tunneling electron excites a plasmon ① that is absorbed by the suspended emitter ②. Eventually, the excited emitter emits a photon ③. (c)–(f) Spectra of different copolymer junctions with their respective plasmon spectra (the blue line) recorded with the metal tip in front of the bare Au(111) prior to the formation of a molecular junction.

Conversely, Figs. 4(e) and 4(f) show that the intensities of the vibronic peaks with respect to the 0–0 line are reduced if the plasmon is intense at the corresponding energies. This ratio is independent of the excitation rate since all of these lines pertain to the same initial excited state. The variation of this ratio therefore informs us of how Q is affected by the plasmon intensity. Q is reduced here by the presence of intense plasmon resonances, a behavior indicating that the plasmonic cavity provides nonradiative decay channels for the molecular exciton. Similar behaviors were reported in photoluminescence measurements of single-molecule emitters having a high intrinsic quantum yield [38]. Overall, our data show that the surface plasmons enhance the excitation rate of the suspended emitter but reduce its probability to decay radiatively. This also confirms that the highly coherent excited state of our single-molecule junction can be efficiently transferred to the plasmons in a nonradiative decay of the molecular exciton, a necessary condition for future hybrid electronic-plasmonic circuits integrating single molecules as controllable transducer. We believe that the narrow linewidth of this molecular source will enable quantum communication experiments and applications with electrically gated plasmonic circuits.

The authors thank Stéphane Berciaud, Fabrice Charra, and Laurent Limot for the stimulating discussions, and Virginie Speisser, Jean-Georges Faullumel, Michelangelo Romeo, and Olivier Crégut for the technical support. This work was performed using HPC resources from GENCI-IDRIS (Grant No. 2015097459). The Agence National de la Recherche (Project SMALL'LED No. ANR-14-CE26-0016-01), the Labex NIE (Contract No. ANR-11-LABX-0058_NIE), and the Région Alsace and the International Center for Frontier Research in Chemistry (FRC) are acknowledged for their financial support.

*guillaume.schull@ipcms.unistra.fr

[1] R. J. Walters, R. V. A. van Loon, I. Brunets, J. Schmitz, and A. Polman, Nat. Mater. **9**, 21 (2010).
[2] D. Y. Fedyanin, A. V. Krasavin, A. V. Arsenin, and A. V. Zayats, Nano Lett. **12**, 2459 (2012).
[3] K. C. Y. Huang, M.-K. Seo, T. Sarmiento, Y. Huo, J. S. Harris, and M. L. Brongersma, Nat. Photonics **8**, 244 (2014).
[4] P. Rai, N. Hartmann, J. Berthelot, J. Arocas, G. Colas des Francs, A. Hartschuh, and A. Bouhelier, Phys. Rev. Lett. **111**, 026804 (2013).
[5] R. Berndt, J. K. Gimzewski, and P. Johansson, Phys. Rev. Lett. **67**, 3796 (1991).
[6] T. Wang, E. Boer-Duchemin, Y. Zhang, G. Comtet, and G. Dujardin, Nanotechnology **22**, 175201 (2011).
[7] P. Bharadwaj, A. Bouhelier, and L. Novotny, Phys. Rev. Lett. **106**, 226802 (2011).
[8] Z. Dong, H.-S. Chu, D. Zhu, W. Du, Y. A. Akimov, W. P. Goh, T. Wang, K. E. J. Goh, C. Troadec, C. A. Nijhuis, and J. K. W. Yang, ACS Photonics **2**, 385 (2015).
[9] C. Große, A. Kabakchiev, T. Lutz, R. Froidevaux, F. Schramm, M. Ruben, M. Etzkorn, U. Schlickum, K. Kuhnke, and K. Kern, Nano Lett. **14**, 5693 (2014).
[10] C. Brunel, B. Lounis, P. Tamarat, and M. Orrit, Phys. Rev. Lett. **83**, 2722 (1999).
[11] B. Lounis and W. Moerner, Nature (London) **407**, 491 (2000).
[12] J. Michaelis, C. Hettich, J. Mlynek, and V. Sandoghdar, Nature (London) **405**, 325 (2000).
[13] X. H. Qiu, G. V. Nazin, and W. Ho, Science **299**, 542 (2003).
[14] P. Avouris and B. N. J. Persson, J. Phys. Chem. **88**, 837 (1984).
[15] N. L. Schneider, J. T. Lü, M. Brandbyge, and R. Berndt, Phys. Rev. Lett. **109**, 186601 (2012).
[16] G. Reecht, F. Scheurer, V. Speisser, Y. J. Dappe, F. Mathevet, and G. Schull, Phys. Rev. Lett. **112**, 047403 (2014).

[17] C. W. Marquardt, S. Grunder, A. Blaszczyk, S. Dehm, F. Hennrich, H. v. Lohneysen, M. Mayor, and R. Krupke, Nat. Nanotechnol. **5**, 863 (2010).

[18] See Supplemental Material at http://link.aps.org/supplemental/10.1103/PhysRevLett.116.036802, which includes Refs. [19–22], for for details regarding S1, the experimental setup S2, the on-surface polymerization products S3, the experimental procedure used to lift a molecular wire in the STM junction S4, the TD-DFT simulations of the excited and ground states S5, the DFT simulations of the Raman spectra S6, vibronic spectra of different emitters S7, the experimental determination of γ_{exc} vs $E(r, h\nu)$.

[19] J. G. Keizer, J. K. Garleff, and P. M. Koenraad, Rev. Sci. Instrum. **80**, 123704 (2009).

[20] L. Lafferentz, F. Ample, H. Yu, S. Hecht, C. Joachim, and L. Grill, Science **323**, 1193 (2009).

[21] M. J. Frisch *et al.*, *Gaussian 09, Revision B.01* (Gaussian, Inc., Wallingford, CT, 2009).

[22] K. Meguro, K. Sakamoto, R. Arafune, M. Satoh, and S. Ushioda, Phys. Rev. B **65**, 165405 (2002).

[23] L. Grill, M. Dyer, L. Lafferentz, M. Persson, M. V. Peters, and S. Hecht, Nat. Nanotechnol. **2**, 687 (2007).

[24] L. Lafferentz, V. Eberhardt, C. Dri, C. Africh, G. Comelli, F. Esch, S. Hecht, and L. Grill, Nat. Chem. **4**, 215 (2012).

[25] A. Wiengarten, J. A. Lloyd, K. Seufert, J. Reichert, W. Auwärter, R. Han, D. A. Duncan, F. Allegretti, S. Fischer, S. C. Oh, O. Saglam, L. Jiang, S. Vijayaraghavan, D. Écija, A. C. Papageorgiou, and J. V. Barth, Chem. Eur. J. **21**, 12285 (2015).

[26] We attribute the 40 meV scattering of the 0–0 line energy to tiny changes of the porphyrin-thiophene and thiophene-electrode couplings from junction to junction.

[27] S. W. Wu, G. V. Nazin, and W. Ho, Phys. Rev. B **77**, 205430 (2008).

[28] Z. C. Dong, X. L. Zhang, H. Y. Gao, Y. Luo, C. Zhang, L. G. Chen, R. Zhang, X. T. Y. Zhang, J. L. Yang, and J. G. Hou, Nat. Photonics **4**, 50 (2010).

[29] C. Galland, A. Högele, H. E. Türeci, and A. Imamoğlu, Phys. Rev. Lett. **101**, 067402 (2008).

[30] J. T. Hugall and J. J. Baumberg, Nano Lett. **15**, 2600 (2015).

[31] S.-E. Zhu, Y.-M. Kuang, F. Geng, J.-Z. Zhu, C.-Z. Wang, Y.-J. Yu, Y. Luo, Y. Xiao, K.-Q. Liu, Q.-S. Meng, L. Zhang, S. Jiang, Y. Zhang, G.-W. Wang, Z.-C. Dong, and J. G. Hou, J. Am. Chem. Soc. **135**, 15794 (2013).

[32] L. Fleury, P. Tamarat, B. Lounis, J. Bernard, and M. Orrit, Chem. Phys. Lett. **236**, 87 (1995).

[33] R. Zhang, Y. Zhang, Z. C. Dong, S. Jiang, C. Zhang, L. G. Chen, L. Zhang, Y. Liao, J. Aizpurua, Y. Luo, J. L. Yang, and J. G. Hou, Nature (London) **498**, 82 (2013).

[34] J. Lee, S. M. Perdue, A. Rodriguez Perez, and V. A. Apkarian, ACS Nano **8**, 54 (2014).

[35] N. L. Schneider and R. Berndt, Phys. Rev. B **86**, 035445 (2012).

[36] G. Tian, J.-C. Liu, and Y. Luo, Phys. Rev. Lett. **106**, 177401 (2011).

[37] K. Miwa, M. Sakaue, B. Gumhalter, and H. Kasai, J. Phys. Condens. Matter **26**, 222001 (2014).

[38] P. Anger, P. Bharadwaj, and L. Novotny, Phys. Rev. Lett. **96**, 113002 (2006).